1063

NASA Contractor Report 177956

PREDICTION OF FAR FIELD NOISE

FROM WIND ENERGY FARMS

Kevin P. Shepherd and Harvey H. Hubbard

THE BIONETICS CORPORATION
Hampton, Virginia

NASA

National Aeronautics and
Space Administration

Langley Research Center
Hampton, Virginia 23665

TABLE OF CONTENTS

INTRODUCTION

Wind turbine generators are being grouped in large numbers to establish wind energy farms and there is concern for possible adverse environmental impact of the radiated noise on nearby residents. Thus there is a need for generally accepted methods for predicting the noise from such wind energy farms for a variety of configurations and operating conditions.

The present paper includes a review of the basic physical factors involved in making predictions; and outlines an approach which allows for differences in the wind turbine generators, configurations of the wind energy farms and propagation conditions. Example calculations are presented to illustrate the sensitivity of the radiated noise to such variables as machine size, spacing and numbers; and such atmospheric variables as relative humidity, temperature, wind velocity and wind direction.

This effort is part of the Department of Energy program managed by the Solar Energy Research Institute.

CALCULATION METHODOLOGY AND ASSUMPTIONS

Relevant characteristics of the noise sources and factors which influence sound propagation are reviewed and evaluated. Included are such items as the reference noise spectrum for the particular machine used, the directivity of the noise source, atmospheric attenuation, frequency weighting considerations and the geometric arrangement of the wind energy farm. The methodology used to predict the noise from a large number of sources such as a wind energy farm is described along with the simplifying assumptions which are valid and pertinent.

Single Machine Reference Spectrum

The most basic information required for the prediction of noise from a wind energy farm is the noise output of a single machine. Its noise spectrum may be predicted based on knowledge of the geometry and operating conditions of the machine (refs. 1 and 2) or it may be measured at a reference distance. An example of spectral data for a particular size range of machines is given in figure 1. The measured spectrum is taken from ref. 3 and represents a 50 kw downwind machine having a three blade rotor with a diameter of 56 ft. The hatched area encompasses the range of available unpublished data for several machines rated at 50 to 100 kw for both downwind and upwind configurations, having 2 and 3 bladed rotors with rotor diameters ranging from 48-61 ft. Also shown in figure 1 is the spectrum which is used subsequently in this paper in example calculations to represent a machine having a rated power of approximately 100 kw. It is the straight (solid) line having a decrease in sound pressure level with increasing frequency of 1 dB per one third octave band or 10 dB per decade.

This shape is considered to be generally representative of the aerodynamic noise of wind turbine generators, however predictions for a specific wind energy farm should be based if possible, on data for the particular types of machines of which it is comprised.

Directivity of the Source

Measurements of aerodynamic noise for a number of large horizontal axis wind turbines (refs.4-8) indicate that the source directivity depends on the significant noise generating mechanisms. For broad band noise sources such as those due to inflow turbulence and blade boundary layer/blade trailing edge interactions, the sound pressure level contours are approximately circular at distances close to the machine. The above higher frequency sources are common to all types of machines. Lower frequency impulsive noise which is due to the interactions of the blades with the tower wake, radiates most strongly in the upwind and downwind directions. This latter source is characteristic of machines for which the blades are located downwind of the supporting tower.

Even though most wind turbine sites have a prevailing wind direction, it is not uncommon for the wind vector to vary over a range of 90° in azimuth angle during normal operations. Thus one of the simplifying assumptions made in the calculations to follow is that each individual machine behaves like an omnidirectional acoustic point source.

Spherical Spreading and Atmospheric Absorption

For the case of non-directional single sources and closely grouped multiple sources, spherical spreading may be assumed in the far radiation field. Circular wave fronts propagate in all directions from the source and the sound pressure levels decay at the rate of 6 dB per doubling of distance. This latter decay rate is illustrated by the straight line of figure 2, and is valid for situations where no other attenuation mechanisms are operative.

Absorption of sound by the atmosphere is usually substantial for wind turbine noise and must be considered. The resulting effects are illustrated in figure 2 which shows the decay of sound pressure level with distance for various noise frequencies. The top line, as noted above, represents zero atmospheric absorption, a condition that would apply only for low frequency components. At higher frequencies, as indicated by the dashed lines, the decay in sound pressure level with distance becomes larger.

The curve of figure 3 was plotted from the tabulated values of ref. 9 and details the changes in atmospheric absorption as a function of frequency. For the examples shown later in this paper, the ambient temperature was assumed to be 20°C and the relative humidity was assumed to be 70% (see figure 3). Atmospheric absorption values for other conditions of ambient temperature and relative humidity can be obtained from the extensive tables of ref. 9.

-2-

Refraction

Refraction can cause nonuniform propagation as a function of azimuth angle around a source. An example of the effects of refraction due to a mean wind gradient is given in figure 4 for an elevated point source. Note that in the downwind direction the rays tend to bend toward the ground due to the wind gradient whereas in the upwind direction the rays curve upward away from the ground. This results in the formation of a shadow zone upwind of the source within which the noise is greatly attenuated as a function of distance. In a situation where there is a prevailing wind, refraction effects may thus be used to advantage in the siting of wind energy farms. If however the direction of the wind is variable, this advantage is lost. Note that temperature gradients may also be present and may add to or subtract from the effects due to wind illustrated in figure 4. It is believed that in general wind effects will dominate the temperature effects in noise propagation from wind energy farms.

Frequency Weighting Considerations

For the evaluation of the direct effects of noise on communities the "A"-weighted metric expressed in dB(A) is in widespread use. The nature of this metric is shown in figure 5. The assumed single machine reference spectrum for a distance of 30 m is reproduced from figure 1 as the solid line. The equivalent "A"-weighted spectrum at the same distance is shown as the topmost dashed curve. It can be seen that this particular weighting emphasizes the higher frequencies and de-emphasizes the lower frequencies. At increased distances, as illustrated by the bottom two solid curves, the levels of the higher frequency components decay at a faster rate than those of the lower frequencies, due to atmospheric absorption. The result is that the mid-range of frequencies (100-1000Hz) tend to dominate the "A"-weighted spectrum at large distances. Frequencies higher than 1000Hz will generally not be important at large distances due to the effects of atmospheric absorption. Those frequency components below 100Hz may not be significant for "A"-weighting considerations but they can be significant for indirect effects such as noise induced building vibrations, which occur generally at structural resonances below 100 Hz.

Wind Energy Farm Configurations

A number of different geometric arrangements of multiple noise sources has been considered for the purpose of representing example wind energy farms. These different arrangements are shown schematically in figure 6. Configuration A is the baseline with which the others are compared. It consists of 31 machines per row, each machine having a power of approximately 100 kw, and a rotor diameter of 15 m. The spacing between machines is 30 meters, the total row length is 900 m and the spacing between rows is 200 m. The number of rows was varied from one to eight. Configuration B is comparable to configuration A except that the row spacing is reduced to 100 m.

Configuration C involves machines having 4 times the rated power and the machine separation and row separation distances are twice those of the baseline (config. A).

Configurations D and E both have row lengths that are twice that of the baseline. Because of differences in machine spacing, configuration E has the same total number of machines as the baseline whereas configuration D has twice the total number of machines.

SOUND PRESSURE LEVEL CALCULATIONS

A series of parametric sound pressure level calculations has been performed based on the arrays illustrated in figure 6. For the data of figures 7 through 11 the observer is located on the line of symmetry perpendicular to the rows and the observer distance is measured from the nearest row of machines. In figure 11 the observer is located on the line of symmetry parallel to the rows.

For figures 7 through 12 the sound pressure level values were calculated by summing, on an energy basis, the contributions of each individual machine (see appendix). It was assumed that each machine radiated noise equally in all directions and was represented by the reference spectrum shown in figures 1 and 5. The contribution of each machine was based on its distance to the observer position. The calculation of the total sound pressure level assumed that the sources were incoherent (i.e., random phase). Four values of atmospheric absorption, α, were used in the calculations: 0, 0.10, 0.27, 0.54 dB/100 m. These may be considered to represent one-third octave band center frequencies of 50, 250, 500, and 1000 Hz respectively provided that the temperature is 20°C and the relative humidity is 70% (see figure 3). These frequency values were chosen because they encompass the range believed to be important for evaluating the environmental impact of wind turbine noise in adjacent communities.

Effects of Distance

Figure 7 shows calculated sound pressure level values for configuration A as a function of distance downwind for several different values of atmospheric absorption. Figure 7(a) shows the characteristic spreading from an extended source for zero atmospheric absorption. The decay rate as a function of distance is less than for the single source of figure 2. At intermediate distances the array acts like a line source for which the theoretical decay rate is 3 dB per doubling of distance or 10 dB per decade. Only at the extreme distances, greater than one row length or 900 m, does the decay rate approach the single source value of 6 dB per doubling of distance or 20 dB per decade. For figures 7(b), 7(c), and 7(d) for which the atmospheric absorption is greater than zero the decay rates are obviously greater than for the zero absorption case and increase as the absorption coefficient increases.

-4-

Effects of Additional Rows of Machines

The calculations of figure 7 were made for one, two, four and eight rows of machines, thus illustrating the effect of progressively doubling the number of machines. For the case of zero atmospheric absorption and at receiver distances which are large compared to the array dimensions, a doubling of the number of rows results in an increase in sound pressure level of 3 dB. This simply reflects a doubling of acoustic power. At shorter distances the closest machines dominate, and the additional rows result in only a small increment in the sound pressure level.

In the case of non-zero atmsopheric absorption, the row spacing is significant even at large receiver distances. Doubling the number of rows results in less than a 3 dB increase in sound pressure level. This is particularly apparent at the highest frequencies and for the larger number of rows (figure 6(d)).

Effects of Row Length and Numbers of Machines

The effects on the sound pressure levels of doubling the lengths of the rows is illustrated in figures 8 and 9. In figure 8 comparisons are given between configurations A and E. In configuration E the same numbers of machines are involved but the spacing between machines is increased. Comparative data for a single row and for an array of eight rows are shown for absorption coefficients of 0 and 0.54 dB per 100 m. At extreme distances the same levels are achieved for configurations A and E because there is the same number of machines in each row. At the shorter distances the levels are higher for configuration A because of the closer spacing of the machines.

Figure 9 shows similar data for configurations A and D. For these comparisons the machine spacing is constant and the row lengths are doubled by doubling the numbers of machines per row. For these comparisons the sound pressure levels at the shorter distances are equal because of the equal machine spacing. At extreme distances the levels for configuration D are higher by 3 dB because the numbers of machines per row are doubled.

Effects of Row Spacing

The effects on sound pressure levels of a change in the row spacing is seen in figure 10. Comparisons are shown for configurations A and B for atmospheric absorption values of 0 and 0.54 dB per 100 m, and for arrays of 2 and 8 rows. Configuration B has the same numbers of machines per row but the spacing between rows is half the distance of that for configuration A. At all distances the sound pressure levels are higher for the more compact array. These observed differences are however small at extreme distances.

Effects of Machine Power Rating

Configurations A and C are compared in figure 11 to illustrate the effects of machine power rating. For these comparisons the

machine spacing and row spacing for the larger machines are double those for configuration A. Data are given for atmsopheric absorption coefficients of 0 and 0.54 dB per 100 m and for single rows and arrays of 8 rows. The assumptions are made that the reference spectrum shape for the larger machine is the same as for the smaller machine but that the levels are 6 dB higher (implying four times the acoustic power). For the single row of 16 large machines, the sound pressure levels are about 3 dB higher than for a single row of 31 small machines, due to the fact that the total acoustic power is essentially doubled. For the larger arrays the higher sound pressure levels are also associated with the larger machines, due to the greater acoustic power per row of machines. Different results would be obtained if the larger machines had reference spectra which differ in shape from that of figure 1.

Farm Directivity Considerations

Even though the individual machines have been treated as if they radiate sound equally in all directions, an array of such sources may not have uniform directivity characteristics. Figure 12 shows a comparison of the sound pressure levels for configuration A as viewed from two different directions. Data are presented for an observer located on the line of symmetry perpendicular to the rows, and also for an observer located on the line of symmetry parallel to the rows. These two conditions are referred to as downwind and crosswind, respectively in figure 12. At extreme distances the differences in sound pressure level are small. However at the shorter distances the downwind levels are higher because of the closer spacing of the machines in the row.

Sound Pressure Level Contours

Sound pressure level contours for a wind energy farm have been estimated, and are presented in figure 13. The farm geometry was chosen to be configuration A with five rows of 31 machines each, thus yielding an approximately square array. This results in essentially circular sound pressure level contours.

Figure 13 gives sound pressure level contours of 40, 50 and 60 dB for four values of atmospheric absorption. The contours are circular if there are assumed to be no propagation effects due to the wind gradient. These contours thus represent a worst case scenario. It is readily apparent that the low frequency contours extend to much greater distances than do the high frequency contours.

Under the assumption of a fixed wind direction, the distance to contours in the upwind direction is greatly reduced, as indicated by the dashed curves in figure 13. These upwind contours are derived from computed distances to the acoustic shadow zone and excess attenuation occuring within it (see ref. 8). The formation of an acoustic shadow zone results in greatly reduced distances to particular noise level contours for all frequencies above about 60 Hz.

A more dramatic method of illustrating the differences of figure 13 is to compare the ground areas that are exposed to particular sound pressure levels. Figure 14 presents such data, for the two downwind quadrants only of figure 13, for a range of atmospheric absorption values from 0 to 0.54 dB per 100 m. The most obvious result is that the areas exposed to the lower levels of noise radiation are much larger than those exposed to the higher levels. It can also be seen that the exposed areas decrease rapidly as atmospheric absorption increases. This effect is most noticeable for the lower level contour areas for which large distances are involved.

"A"-Weighted Composite Spectra

The data of figures 7 through 14 are derived for a few selected values of atmospheric absorption and illustrate how the noises from individual machines sum together for various arrays of machines. Figure 15 illustrates the effects of "A"-weighting the composite sound spectrum from wind energy farm configuration A. It can be seen that as for the single machine example of figure 4, at large distances the mid range of frequencies dominate the "A"-weighted spectrum.

CONCLUDING REMARKS

A proposed model to predict noise from wind energy farms is presented. Various assumptions are made concerning characteristics of the noise sources and propagation phenomena. The wind turbines are assumed to be omnidirectional noise sources which add together in random phase. Propagation is assumed to be controlled by spherical spreading and atmospheric absorption, with refraction effects included in the upwing direction.

Very few data are available with which to compare the results of this analytical study. As other data become available it may be shown that other factors such as ground absorption, refraction in the downwind direction and noise source directivity may need to be incorporated as refinements to this model.

REFERENCES

1. Grosveld, F.W.: Prediction of Broadband Noise from Horizontal Axis Wind Turbines. AIAA Journal of Propulsion and Power. Vol. 1, No. 4, July-August 1985.

2. Viterna, L.A.: The NASA-LeRC Wind Turbine Sound Prediction Code. Presented at the Department of Energy Wind Turbine Dynamics Conference 24-27 February 1981, NASA CP 2185, 1981.

3. Hubbard, Harvey H., and Shepherd, Kevin P.: Noise Measurements for Single and Multiple Operation of 50 kw Wind Turbine Generators. NASA CR 166052, December 1982.

4. Shepherd, Kevin P. and Hubbard, Harvey H.: Measurements and Observations of Noise from a 4.2 Megawatt (WTS-4) Wind Turbine Generator. NASA CR 166124, May 1983.

5. Grosveld, F.W., Shepherd, K.P. and Hubbard, H.H.: Measurement and Prediction of Broadband Noise from Large Horizontal Axis Wind Turbine Generators. Presented at NASA/DOE Workshop on Horizontal Axis Wind Turbine Technology, Cleveland, Ohio, May 8-10, 1984.

6. Shepherd, Kevin P. and Hubbard, Harvey H.: Sound Measurements and Observations of the MOD-OA Wind Turbine Generator. NASA CR 165856, February 1982.

7. Hubbard, Harvey H., Shepherd, Kevin P. and Grosveld, F.W.: Sound Measurements of the MOD-2 Wind Turbine Generator. NASA CR 165752, July 1981.

8. Shepherd, Kevin P., and Hubbard, Harvey H.: Sound Propagation Studies for a Large Horizontal Axis Wind Turbine. NASA CR 172564, March 1985.

9. Anonymous: Method for the Calculation of the Absorption of Sound in the Atmosphere. ANSI S1.26, 1978.

10. Rathe, E.J.: Note on Two Common Problems of Sound Propagation. Journal of Sound & Vib., vol. 10, no. 3, 1969.

APPENDIX

CALCULATION OF SOUND PRESSURE LEVEL DUE TO MULTIPLE SOURCES

Two methods are presented for calculating the sound pressure level due to multiple noise sources at any arbitrary receiver distance. Both methods assume that each source radiates equally in all directions and include attenuation due to atmospheric absorption. The first method has no limitations on either the number of machines or their geometric arrangements. The second method (derived from ref. 10) which is computationally more efficient, requires that the sources be approximately equally spaced within rows and that the number of sources per row be greater than three.

Method A. Summation of Contributions from Each Source

The required input is a sound pressure level spectrum, either narrow band or one-third octave band, for a single machine. This spectrum should be measured or predicted for a distance M, meters from the machine, where M is approximately equal to the tower height plus the rotor radius.

The following procedure should be performed for each frequency band:

1. The contribution from a single machine at a distance, R, from a receiver is given by:

$$\text{Sound Pressure Level } S_i = L - 20 \log(R/M) - \alpha R$$

where L is sound pressure level at distance M, and α is atmosperic absorption in dB/m (ref. 9).

Note that α varies as a function of frequency, temperature and relative humidity.

2. Calculate contributions from all other sources as in step 1. The total sound pressure level at a particular receiver location is given by:

$$\text{Total Sound Pressure Level} = 10 \log_{10} \sum_{i=1}^{n} 10^{S_i/10}$$

where n is the number of sources.

This procedure should be repeated for all frequency bands, thus yielding a sound pressure level spectrum at the receiver location. Noise measures such as A-weighted sound pressure level may subsequently be calculated for each receiver location.

Method B. Summation of Contributions from Each Row of Machines

If the sources are arranged in rows, the following procedure reduces the computations required to predict the sound pressure level at a receiver location.

As for Method A, the required input is a sound pressure level spectrum for a single source for a distance M. A finite row of sources, spaced "b" meters apart, results in a sound pressure level at a distance R given by:

Row of machines
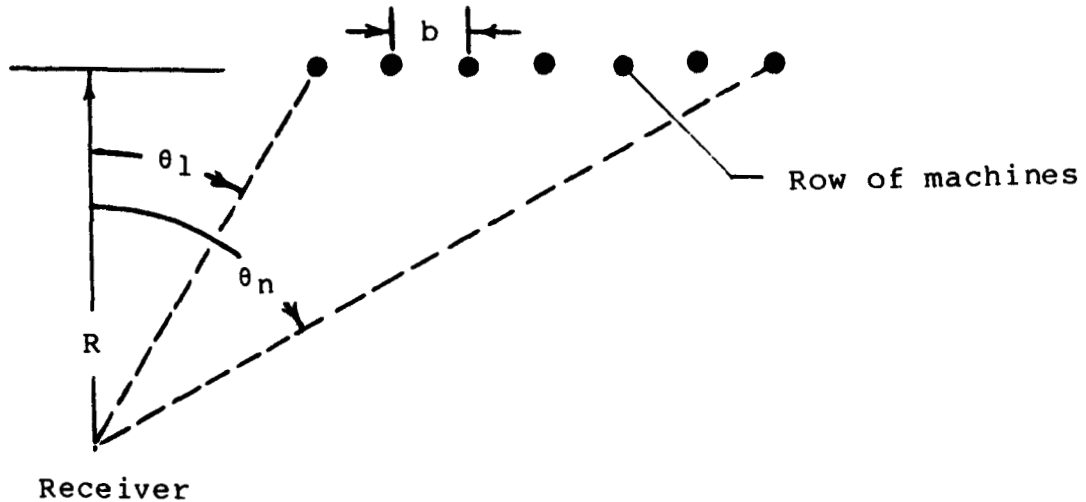
Receiver

$$Si = L + 10 \log_{10} [M^2(\theta_n - \theta_1)/Rb] - \alpha R_1$$

where α is atmospheric absorption in dB/m and R_1 is distance from receiver to closest source.

Note that θ_n, θ_1 are in radians and may take positive or negative values, but θ_n must be greater than θ_1. For the case where the receiver is on the line of symmetry perpendicular to the row, $\theta_1 = -\theta_n$ and $R_1 = R$ and the equation reduces to:

$$Si = L + 10 \log_{10} [2\theta_n M^2/Rb] - \alpha R$$

Contributions from other rows should be calculated similarly and summed as in step 2 of Method A (n will be the number of rows).

This procedure will not work if R=0; however a small number, approaching zero, will overcome this problem. This procedure gives extremely accurate results (errors less than 0.2dB) for atmospheric absorption equal to zero. For non zero absorption values, accuracy is excellent in the downwind direction (perpend-

-10-

icular to rows) but may lead to errors of 1-2dB in the crosswind direction at high frequencies.
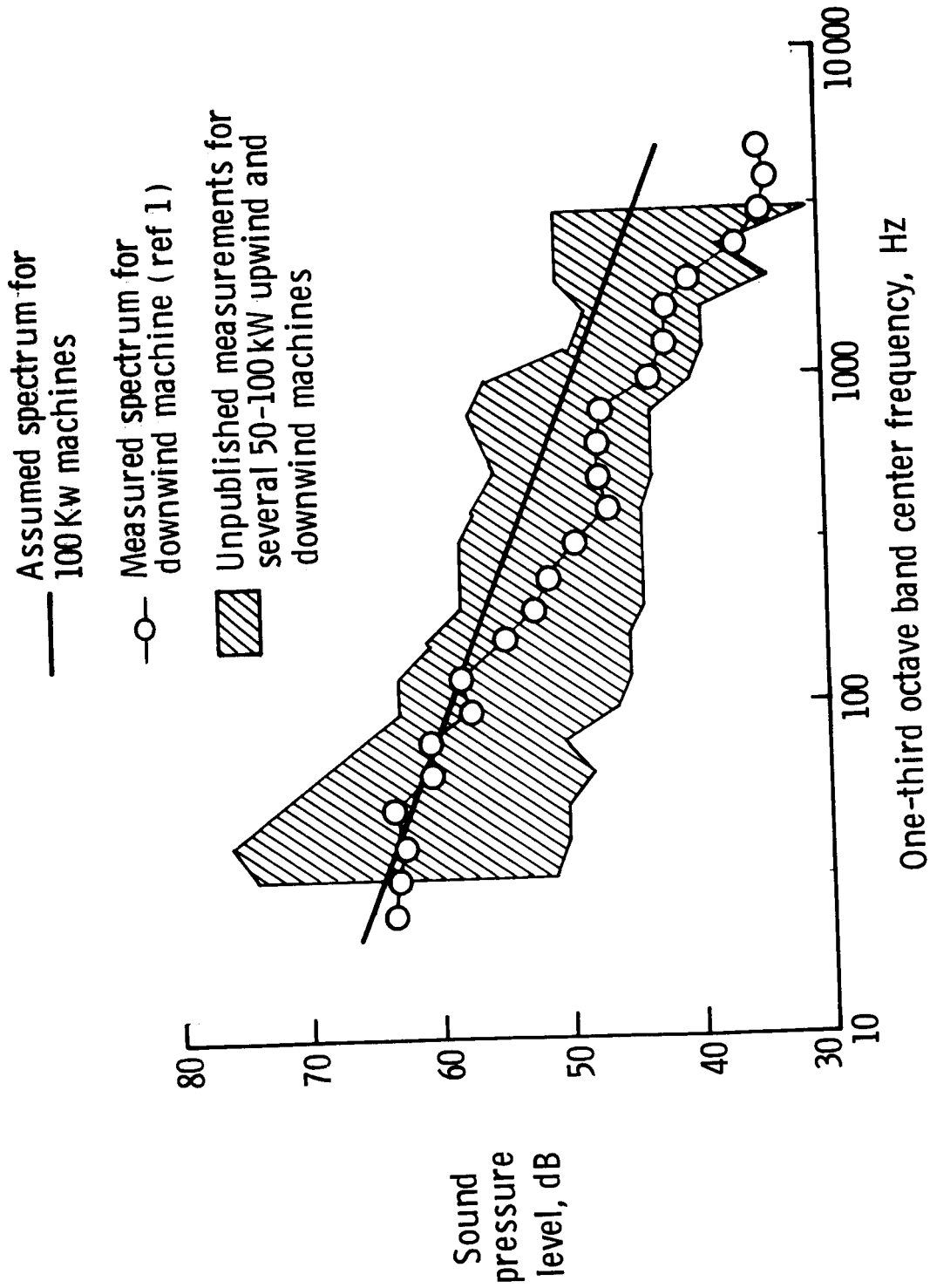
Figure 1. - Noise spectral data at a distance of 30 m downwind at ground level for wind turbines in the 50-100 kw range.
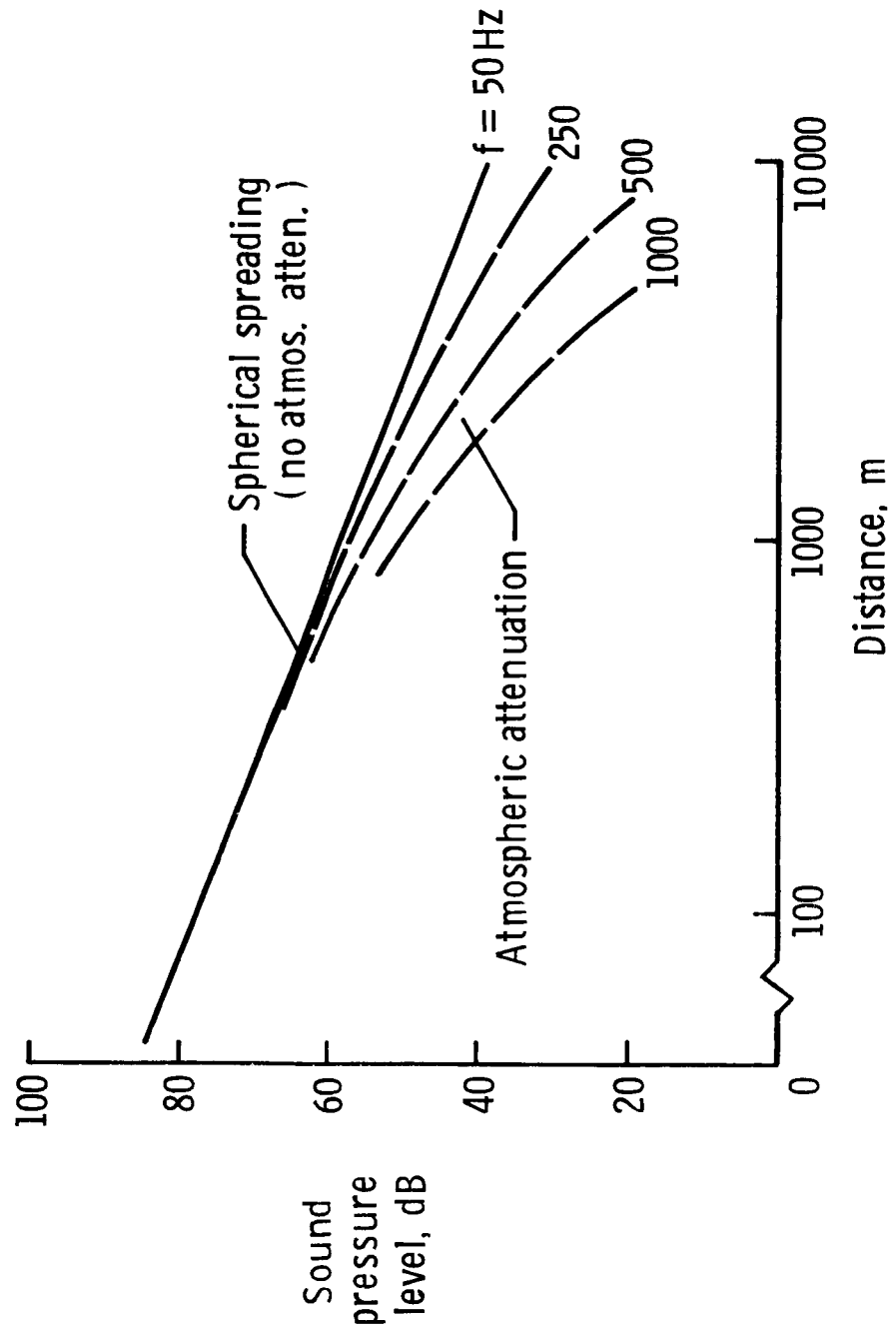
Figure 2. — Sound pressure levels as a function of distance from the source for various one-third octave band center frequencies.
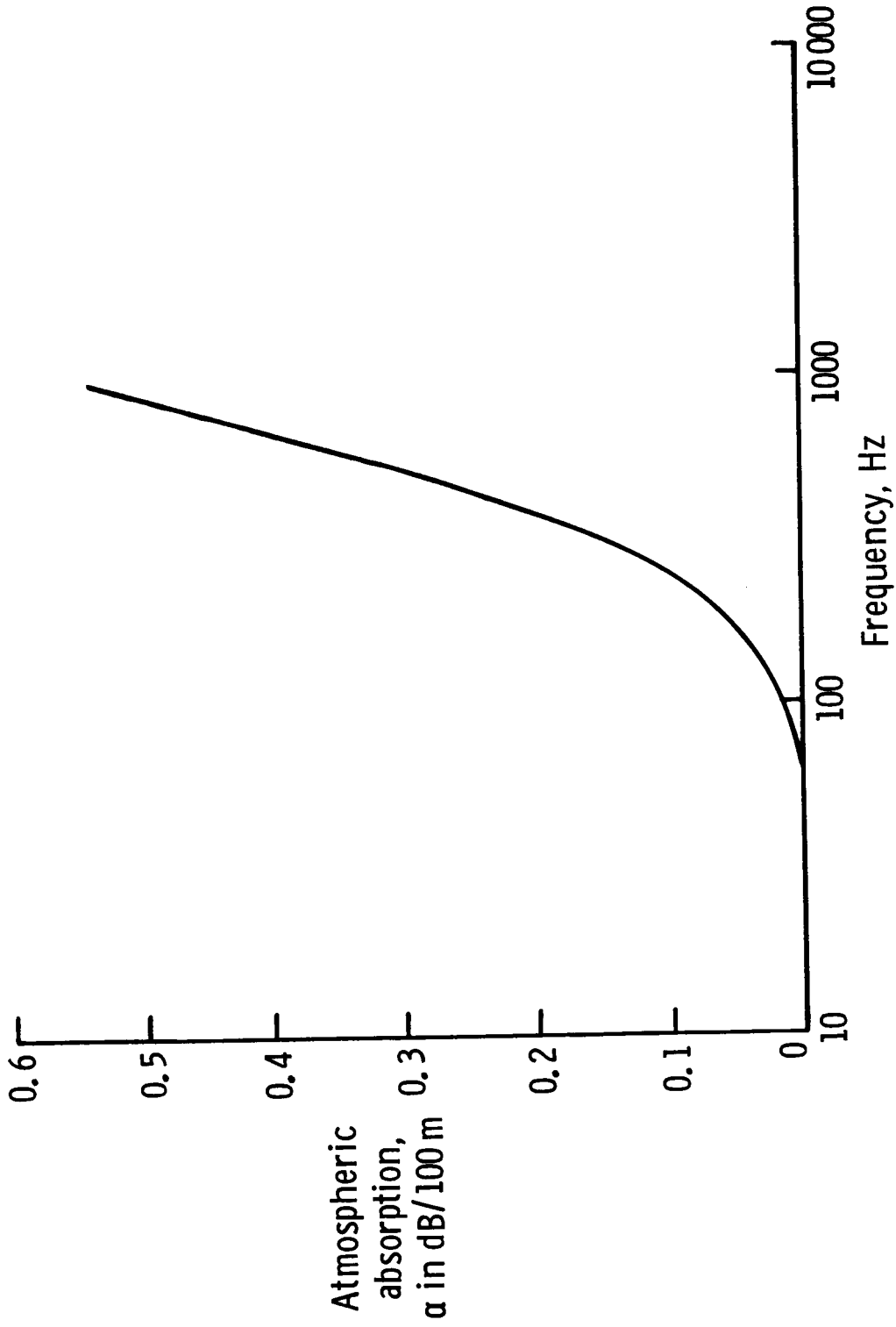
Figure 3. – American national standard values of atmospheric absoprtion in dB/100 m as a function of one-third octave band center frequency. Relative humidity = 70%, ambient temperature = 20°C. (see ref. 9)
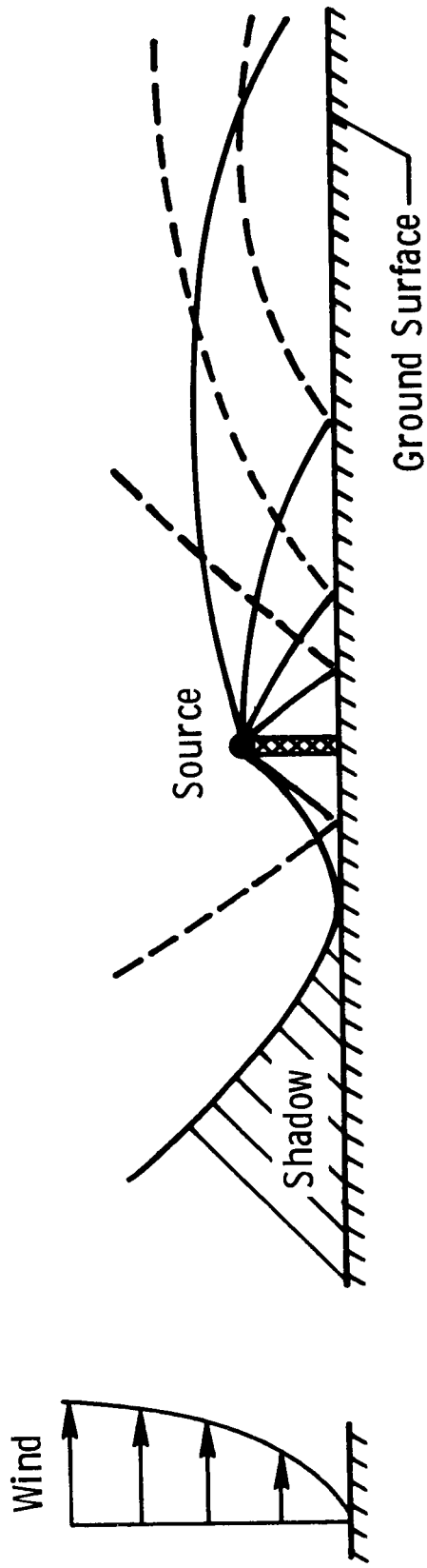
Figure 4. — Ray diagram showing the effects of refraction on the
noise radiation from a point source located above
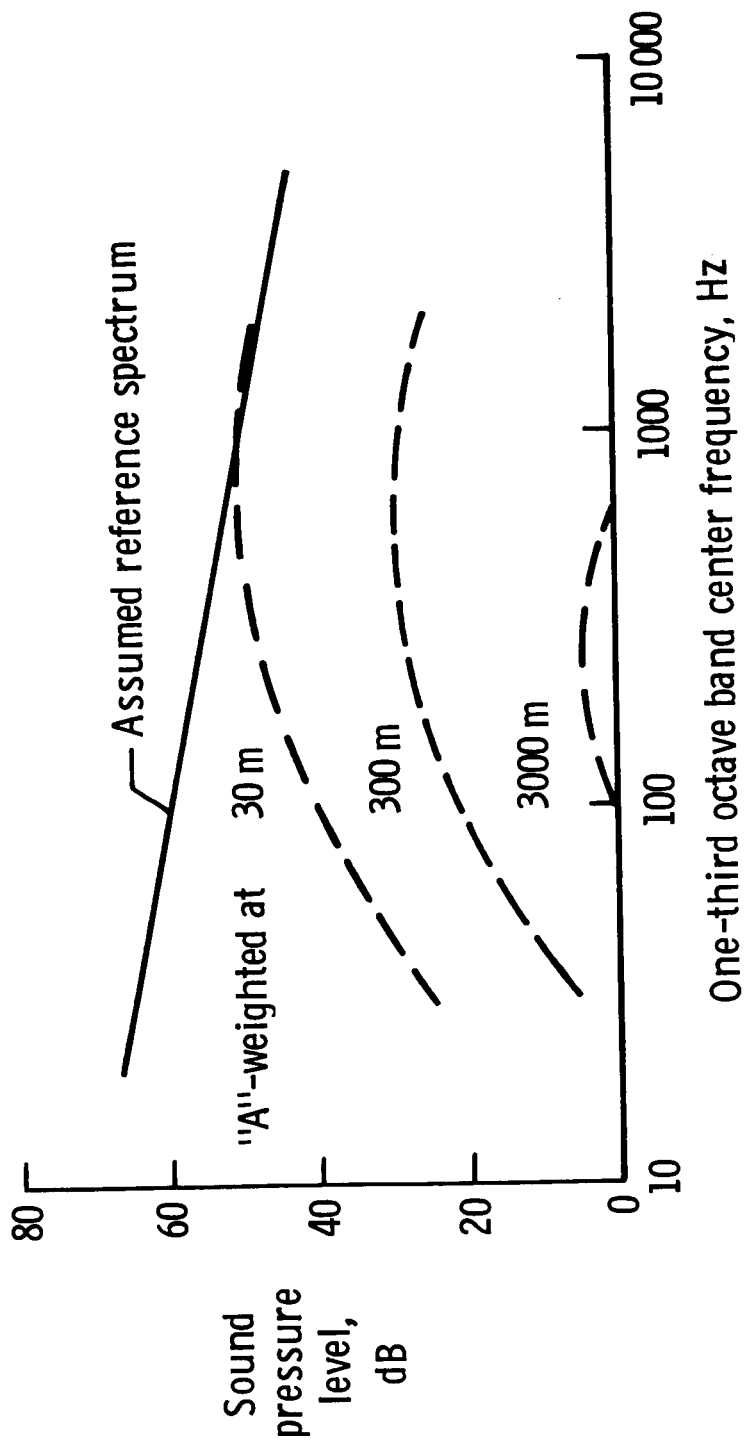ground level in the presence of a mean wind gradient.

Figure 5. – Estimated "A"-weighted noise spectra at various distances downwind from a single machine. D = 15 m, P = 100 kw.
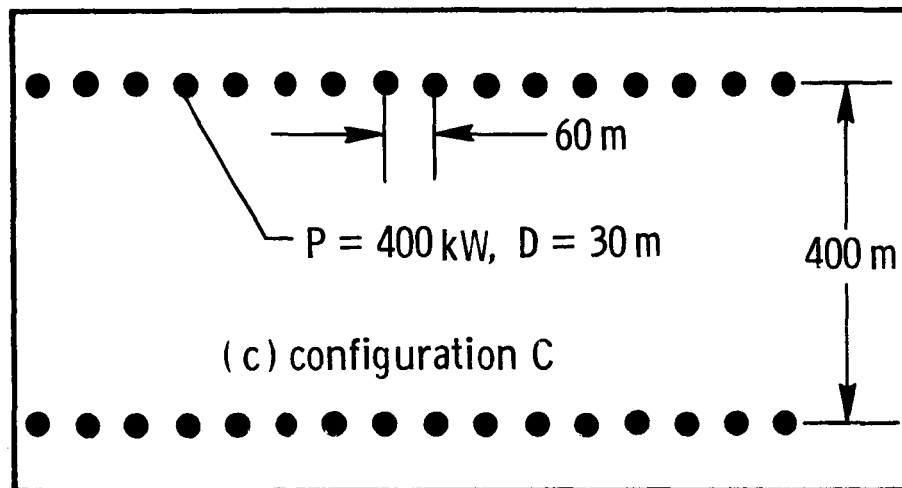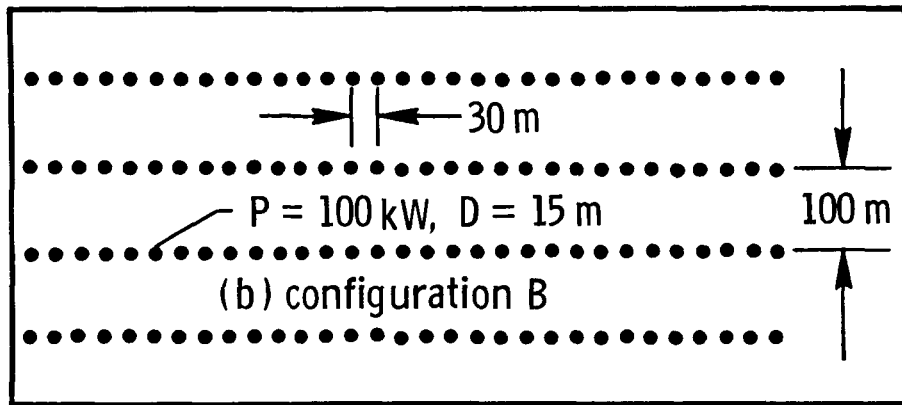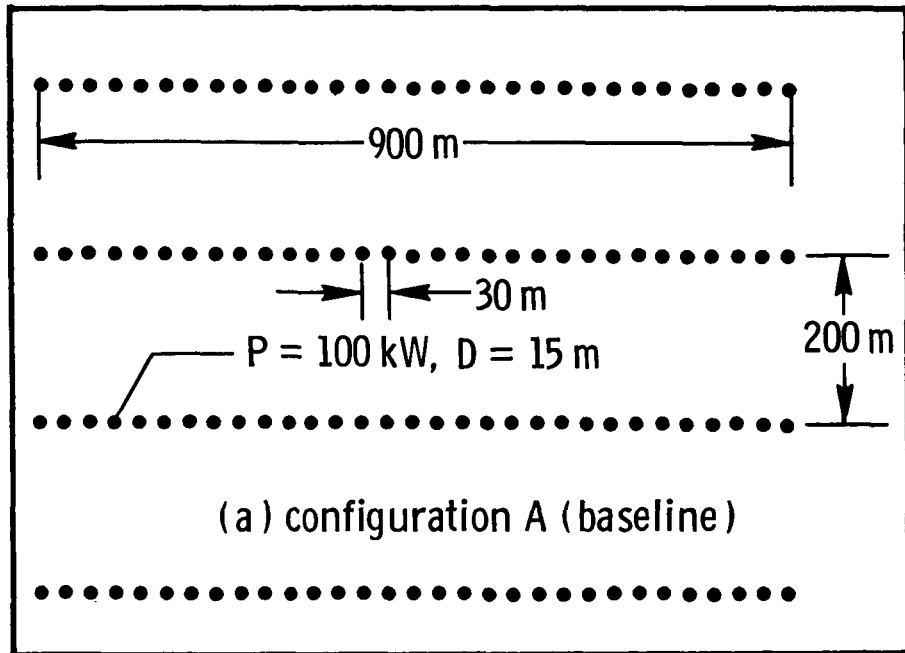
Figure 6. – Schematic diagrams of the geometric layouts of wind energy farms for which noise calculations are presented.

1800 m

30 m

P = 100 kW, D = 15 m

(d) configuration D

60 m
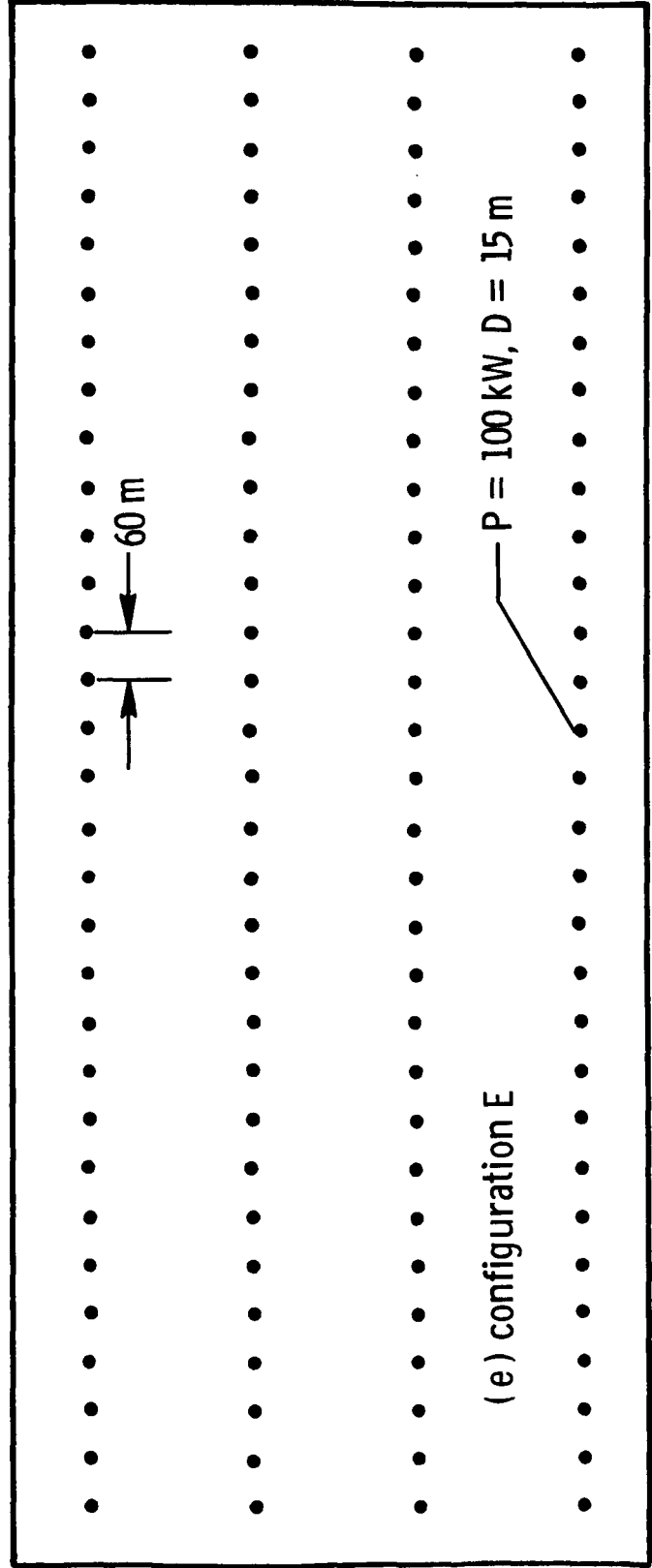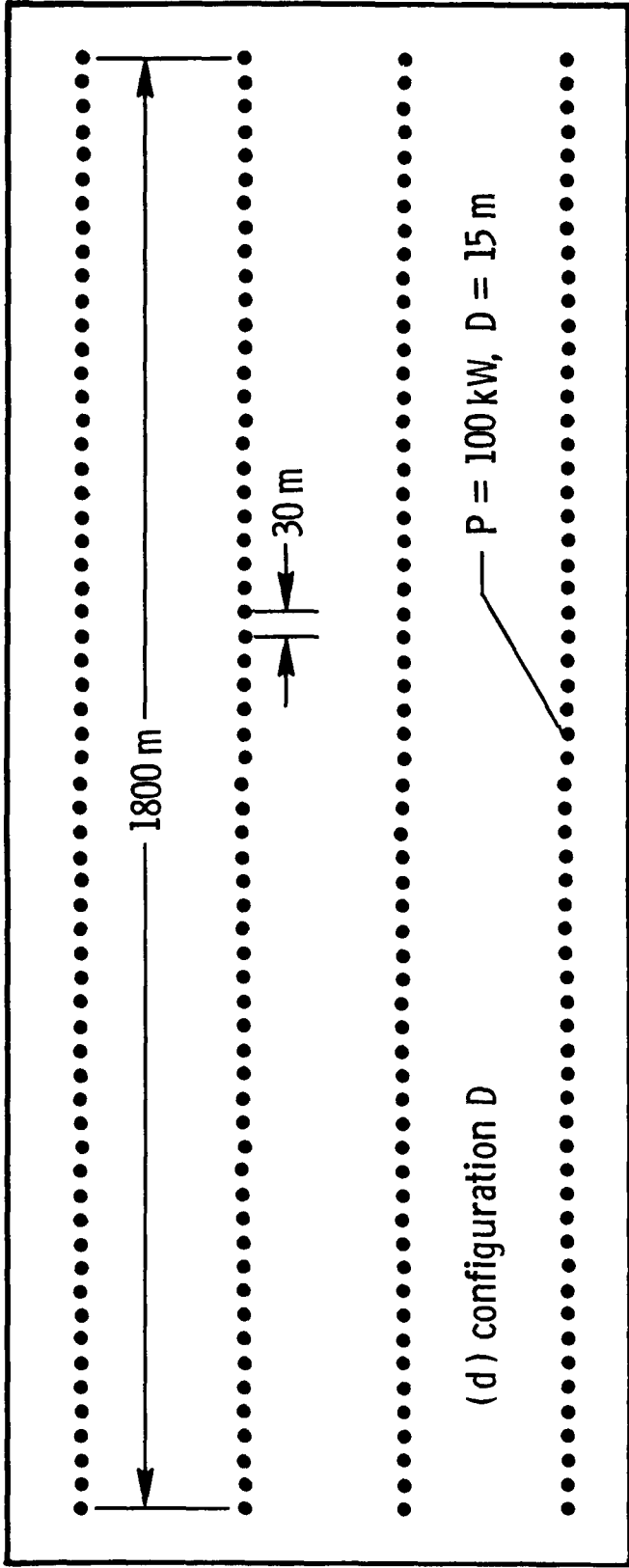
P = 100 kW, D = 15 m
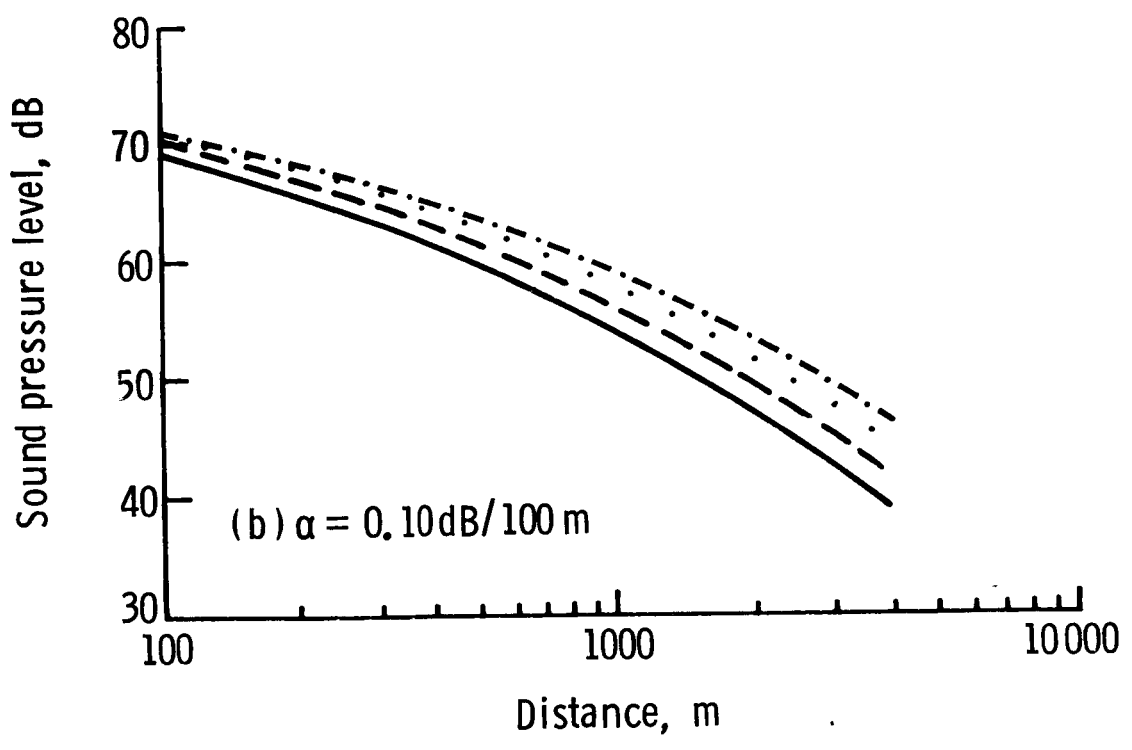
(e) configuration E
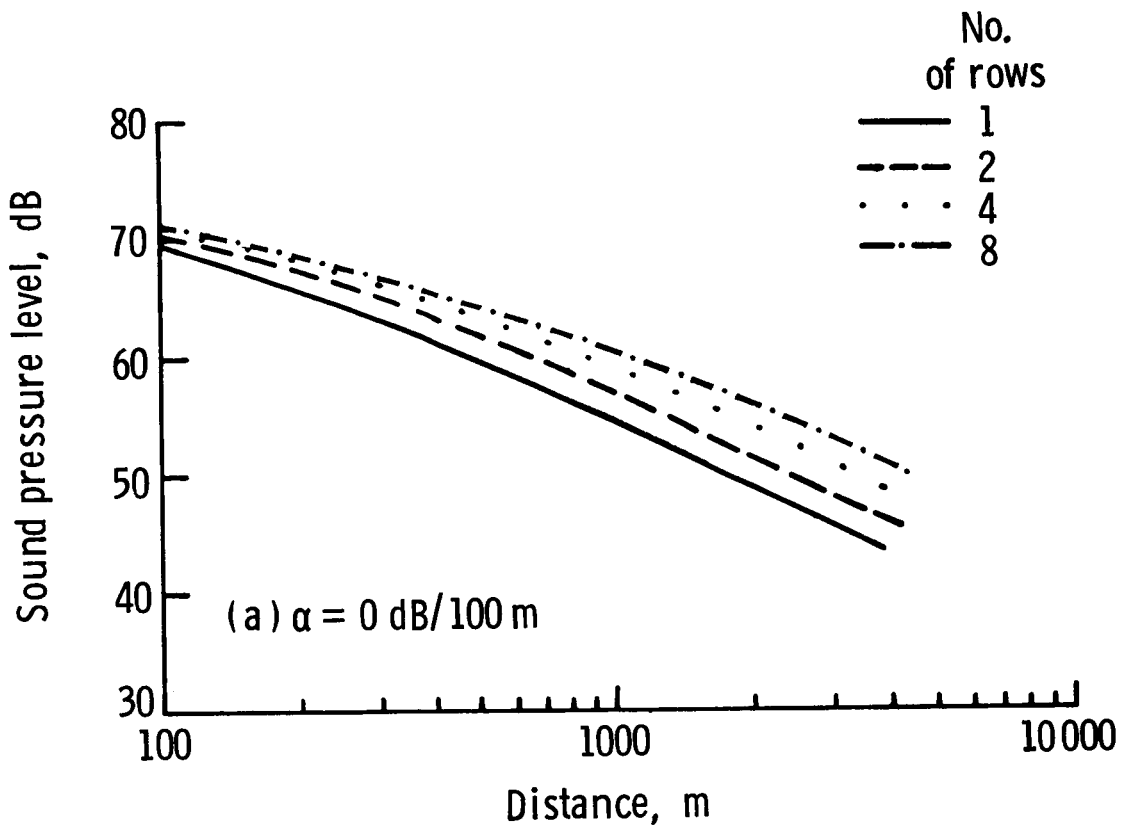
Figure 6. - Concluded.

Figure 7. - Sound pressure levels for various assumed absoprtion
coefficients as a function of distance downwind from
the example wind energy farm of configuration A.

No.
of rows
——— 1
—— — 2
· · · · 4
—·—·— 8

Sound pressure level, dB

80
70
60
50
40
30

(c) $\alpha = 0.27\,dB/100\,m$

100   1000   10 000

Distance, m

Sound pressure level, dB

80
70
60
50
40
30

(d) $\alpha = 0.54\,dB/100\,m$

100   1000   10 000

Distance, m

Figure 7. - Concluded.

	Machines per row	Machine spacing, m	No. of rows
———	31	60	1
— — —	31	30	1
· · · · ·	31	60	8
—·—·—	31	30	8

(a) $\alpha = 0\,dB/100\,m$
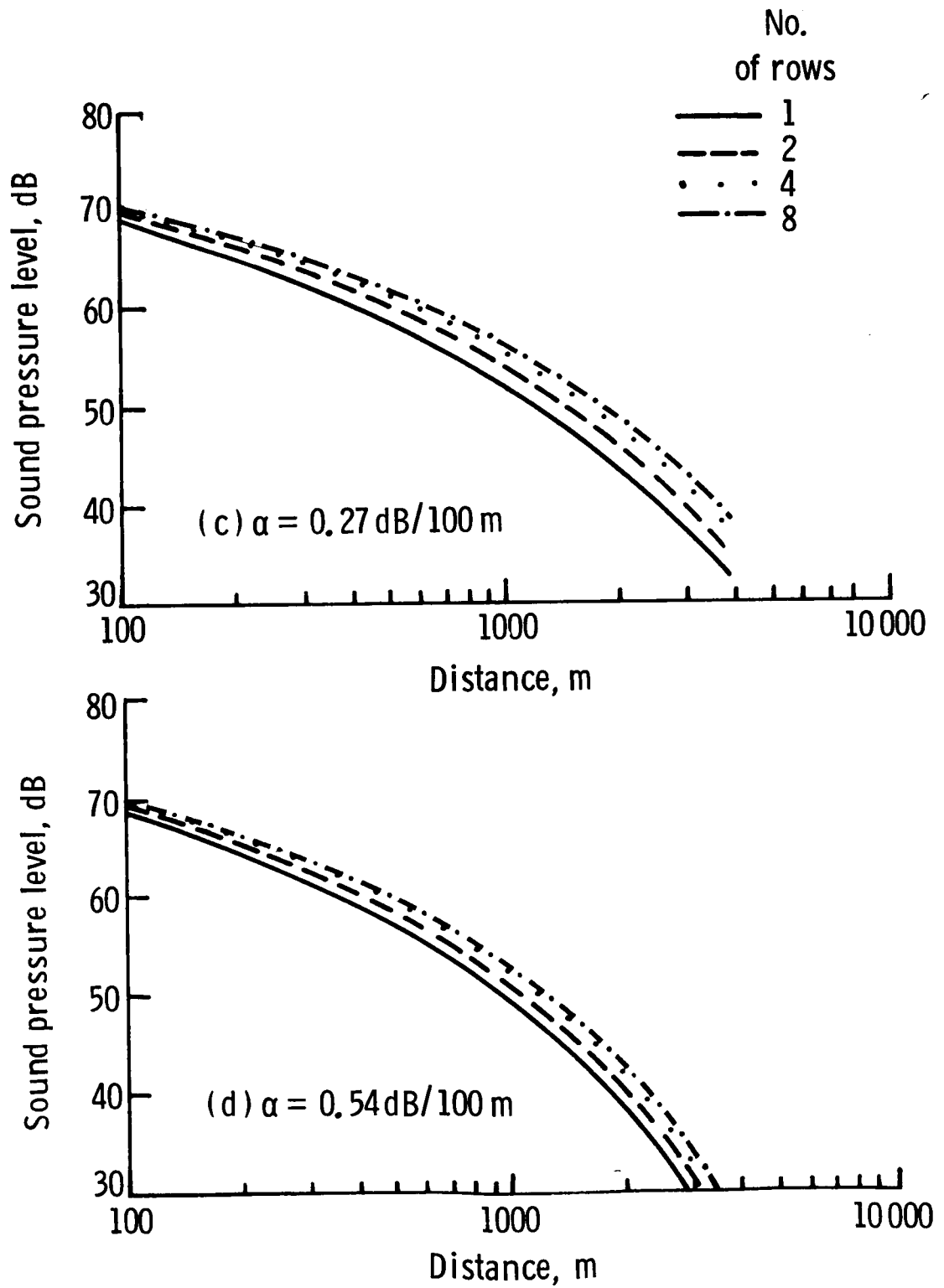
(b) $\alpha = 0.54\,dB/100\,m$
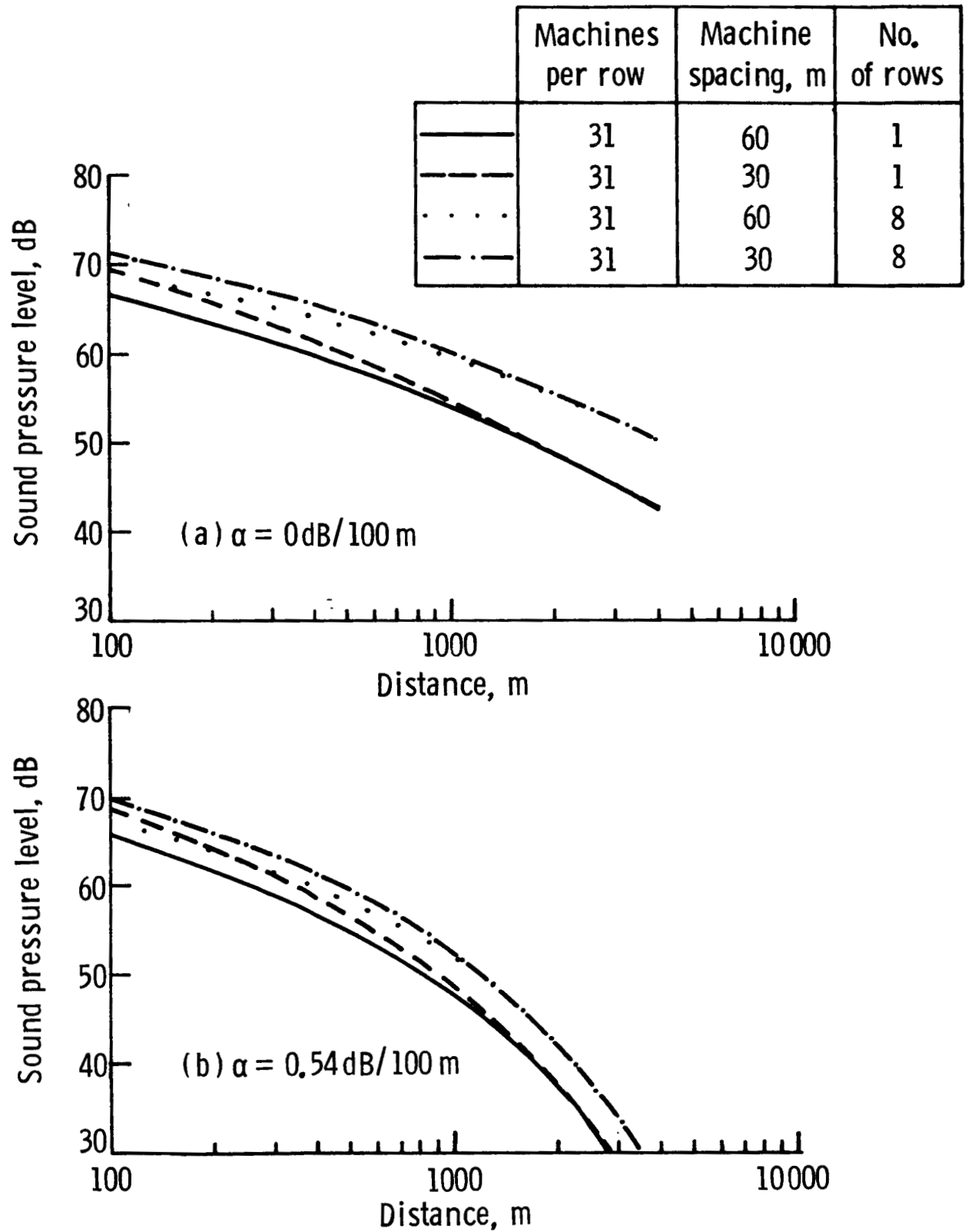
Sound pressure level, dB

Distance, m

Figure 8. – Effects of machine spacing and row length on the
calculated sound pressure levels downwind of wind
energy farms corresponding to configurations A and E.

	Row length, m	Machine spacing, m	No. of rows
——	900	30	1
— · —	1800	30	1
· · · ·	900	30	8
—··—··—	1800	30	8

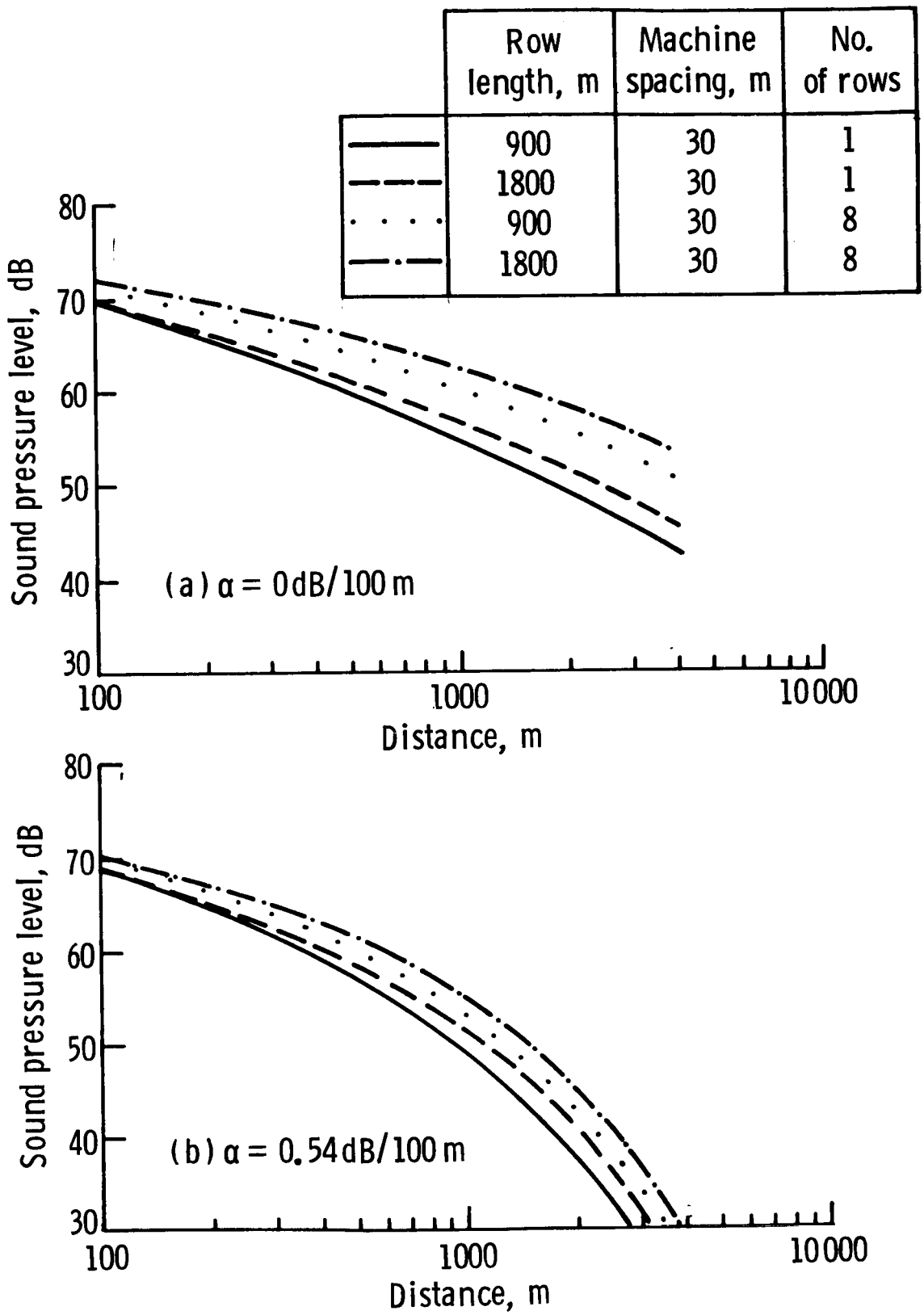(a) $\alpha = 0\,dB/100\,m$

(b) $\alpha = 0.54\,dB/100\,m$

Figure 9. - Effects of row length on the calculated sound pressure levels downwind of wind energy farms corresponding to configurations of A and D.

	Row spacing, m	No. of rows	Machines per row
———	100	2	31
– – –	200	2	31
· · · ·	100	8	31
–·–·–	200	8	31

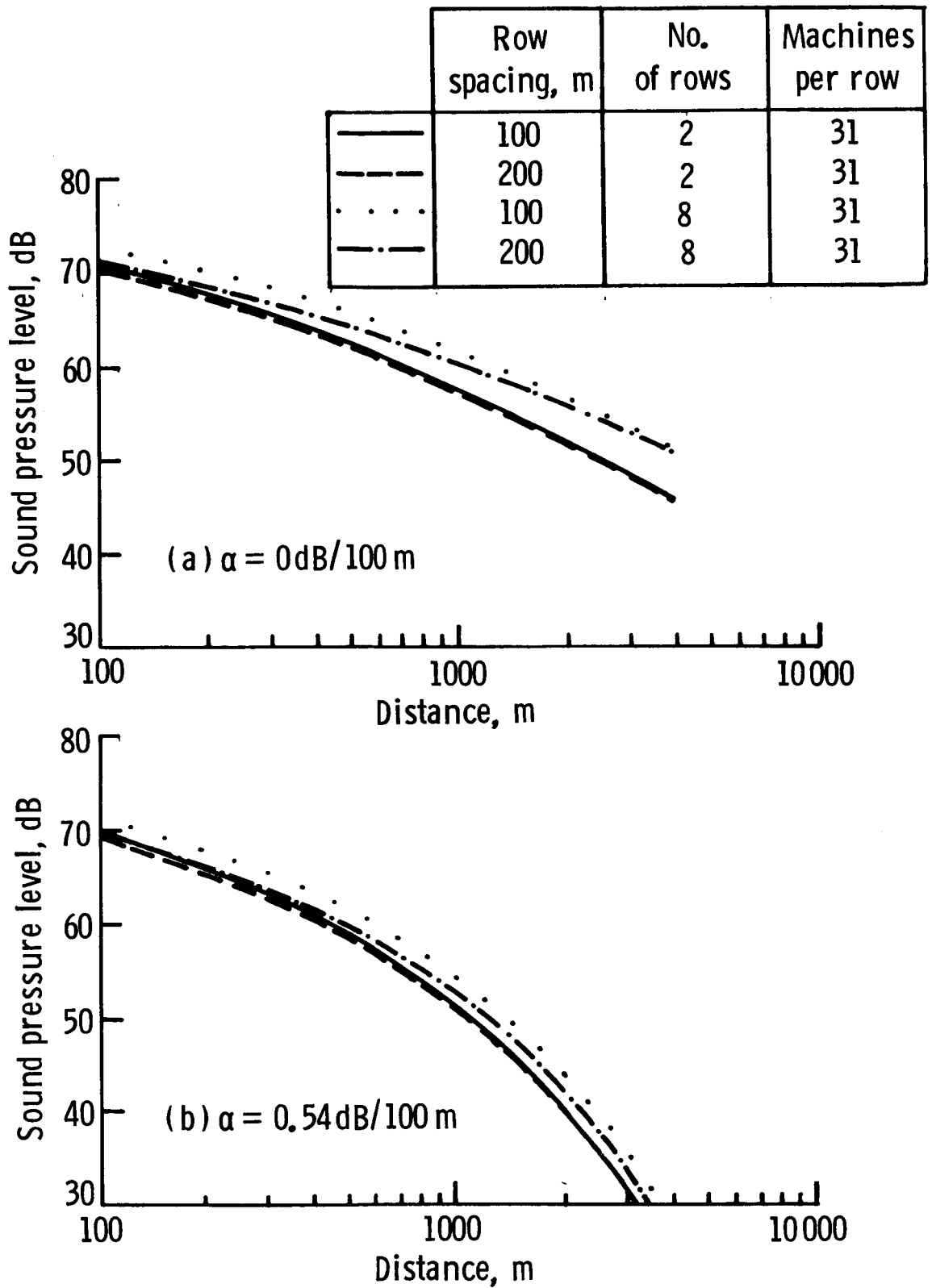(a) $\alpha = 0\,dB/100\,m$

(b) $\alpha = 0.54\,dB/100\,m$

Figure 10. – Effects of row spacing on the calculated sound pressure levels downwind of a wind energy farm corresponding to configurations A and B.

	Machine power, kW	Farm config	No. of rows
——	100	Fig. 5 (a)	1
— · —	400	Fig. 5 (c)	1
· · · ·	100	Fig. 5 (a)	8
— · · —	400	Fig. 5 (c)	8

(a) $f \leq 50\,\mathrm{Hz}$, $\alpha = 0$

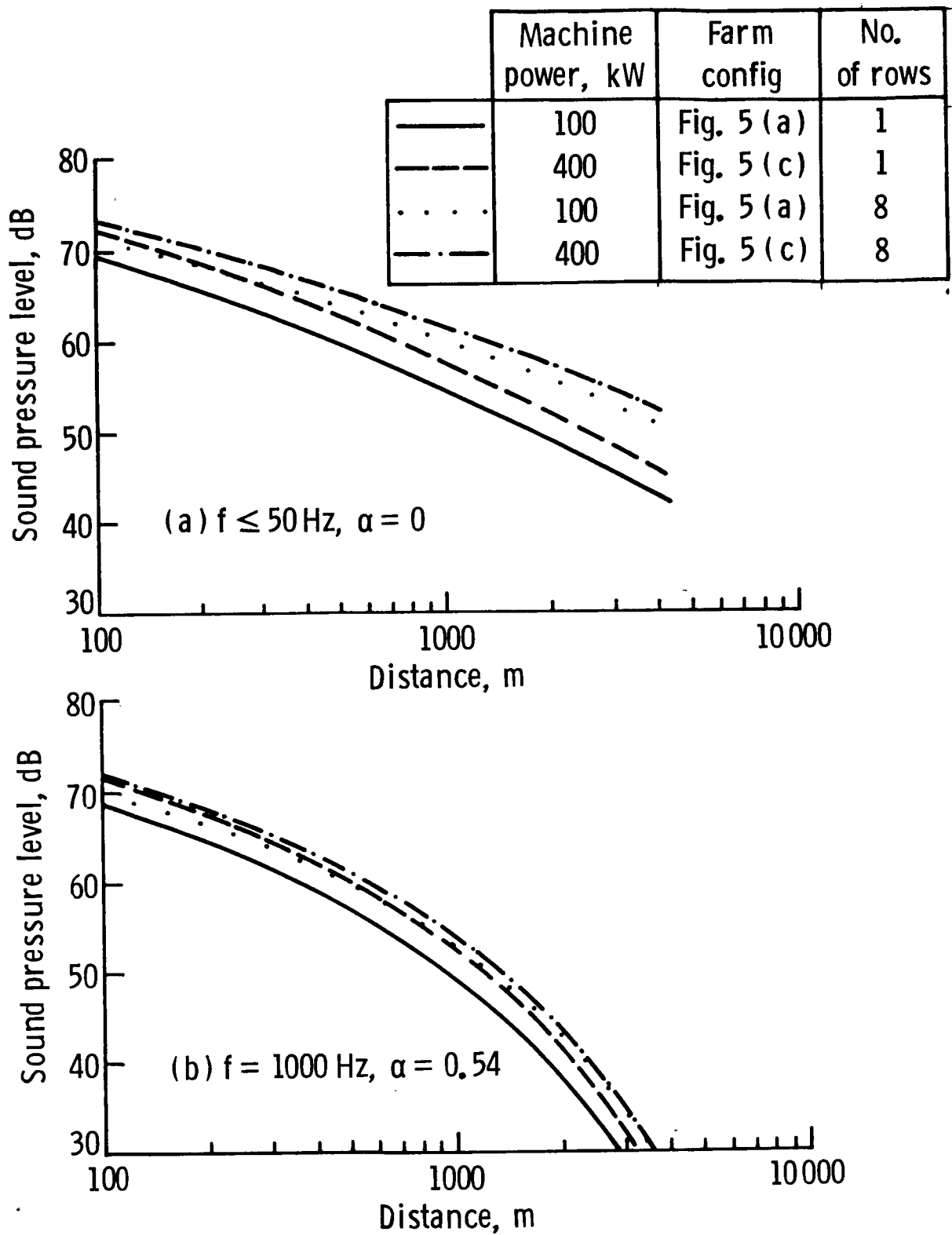(b) $f = 1000\,\mathrm{Hz}$, $\alpha = 0.54$

Figure 11. – Comparisons of sound pressure level as a function of distance in the downwind direction for wind energy farms incorporating two different sizes of machines.
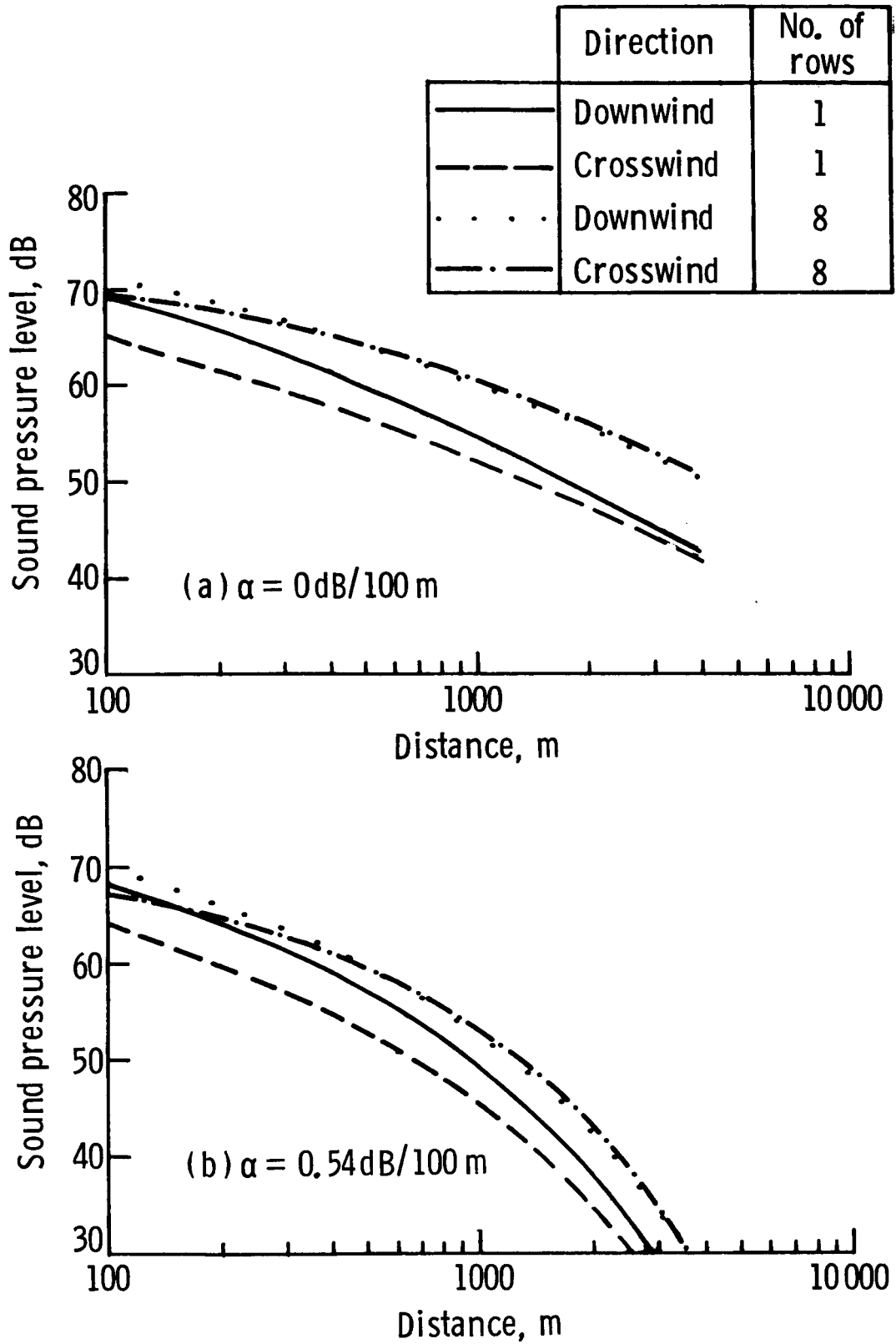
Direction	No. of rows
Downwind	1
Crosswind	1
Downwind	8
Crosswind	8

(a) $\alpha = 0 \, dB/100 \, m$

(b) $\alpha = 0.54 \, dB/100 \, m$

Figure 12. — Comparisons of sound pressure levels as a function
of distance in the downwind and cross wind directions
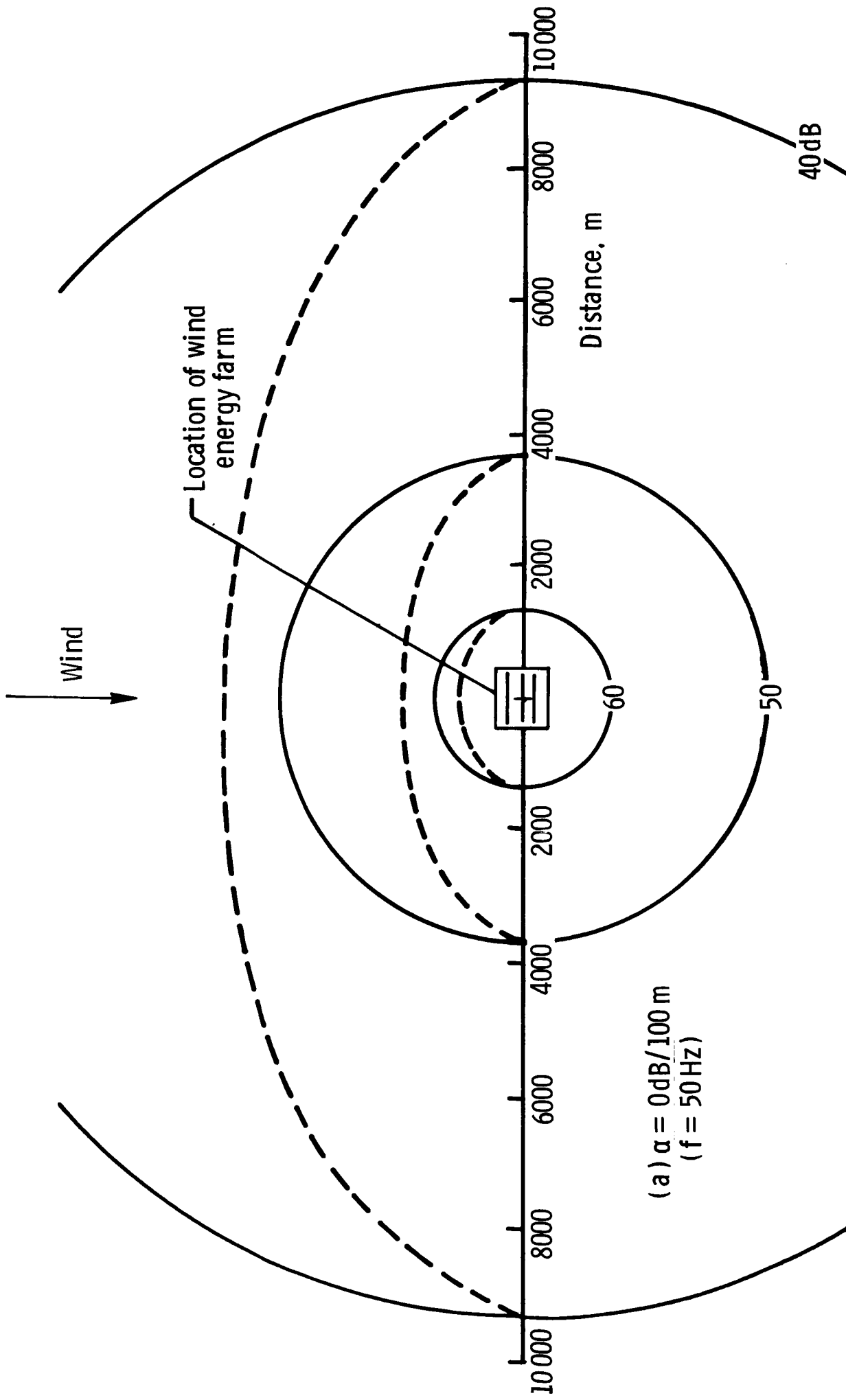from a wind energy farm corresponding to configuration A

Figure 13. – Sound pressure level contours for various assumed absorption coefficients based on an example wind energy farm having 156 machines rated at 100 kW and arranged in 5 rows of 31. S = 30 m, R = 200 m, rel. humidity = 70%. Dashed lines relate to propagation in the upwind direction.

(a) $\alpha = 0\,dB/100\,m$
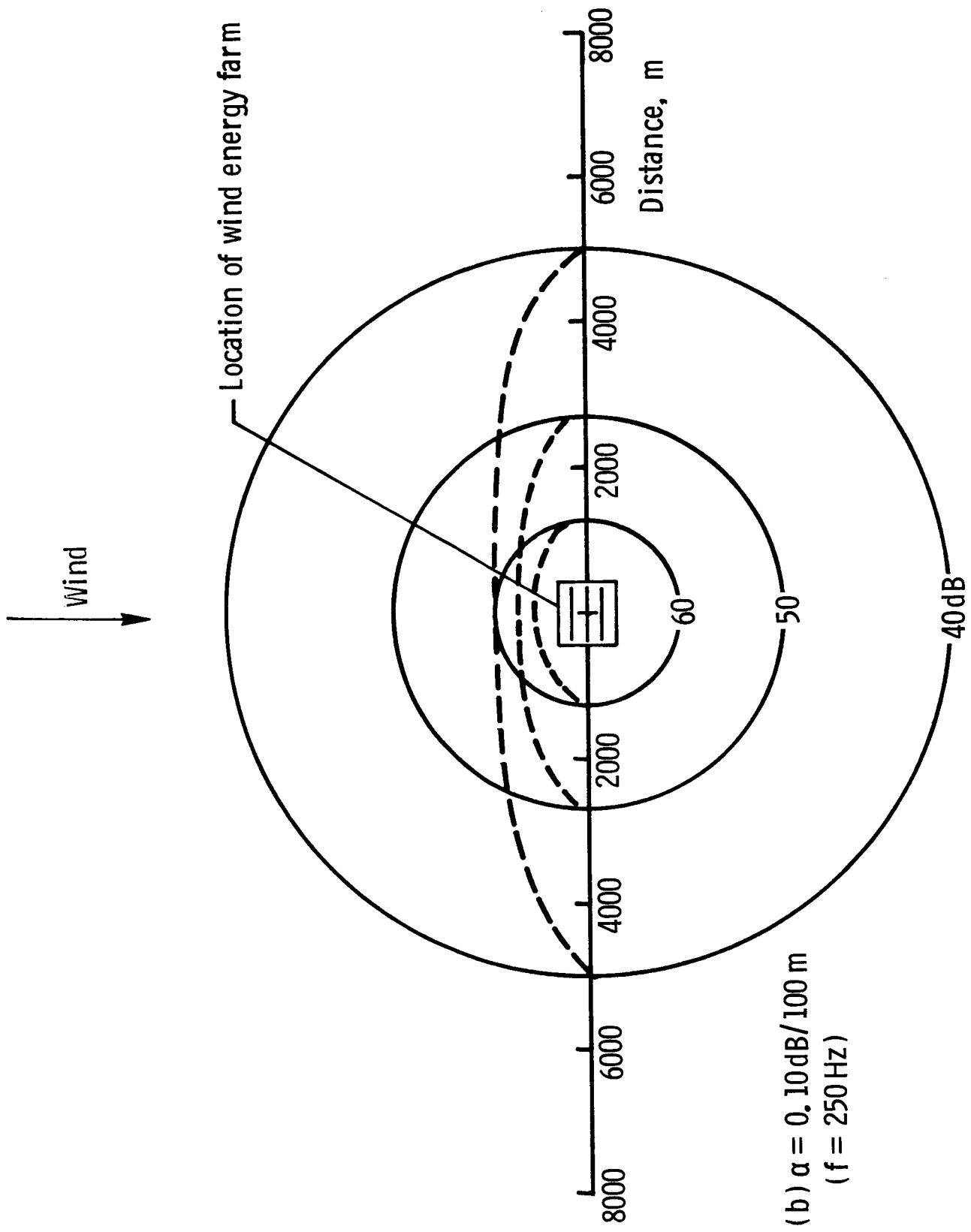(f = 50 Hz)

Wind

Location of wind energy farm

Distance, m

60

50

40dB

(b) $\alpha = 0.10 dB/100 m$
($f = 250 Hz$)

Figure 13. – Continued.

Wind →

Location of wind energy farm

Distance, m

60
50
40 dB

(c) α = 0.27 dB/100 m
(f = 500 Hz)

Figure 13. - Continued.

Wind →

Location of wind energy farm

60
50
40dB

2000
2000

8000   6000   4000   2000
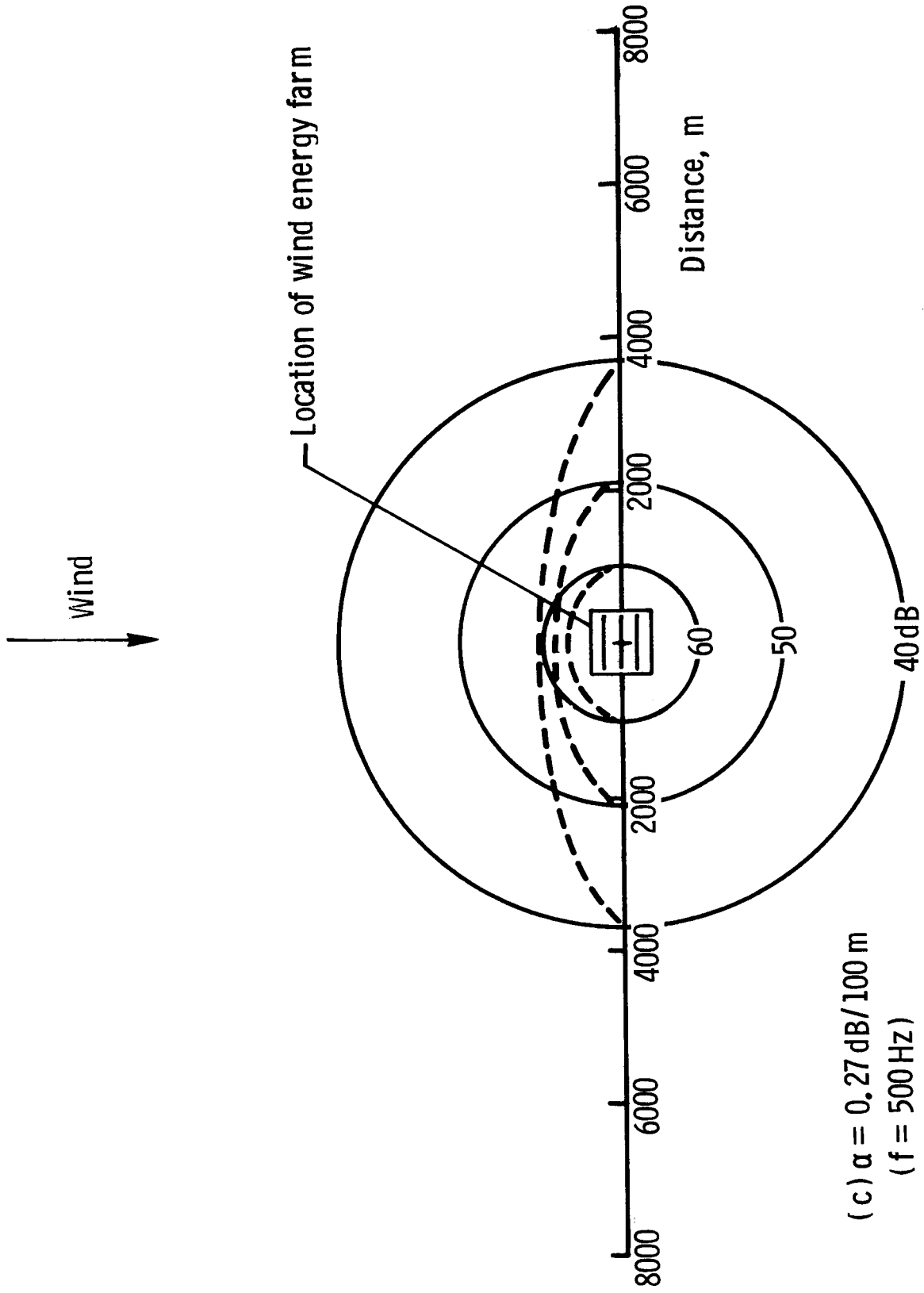
Distance, m

8000   6000   4000

(d) $\alpha = 0.54$ dB/100 m
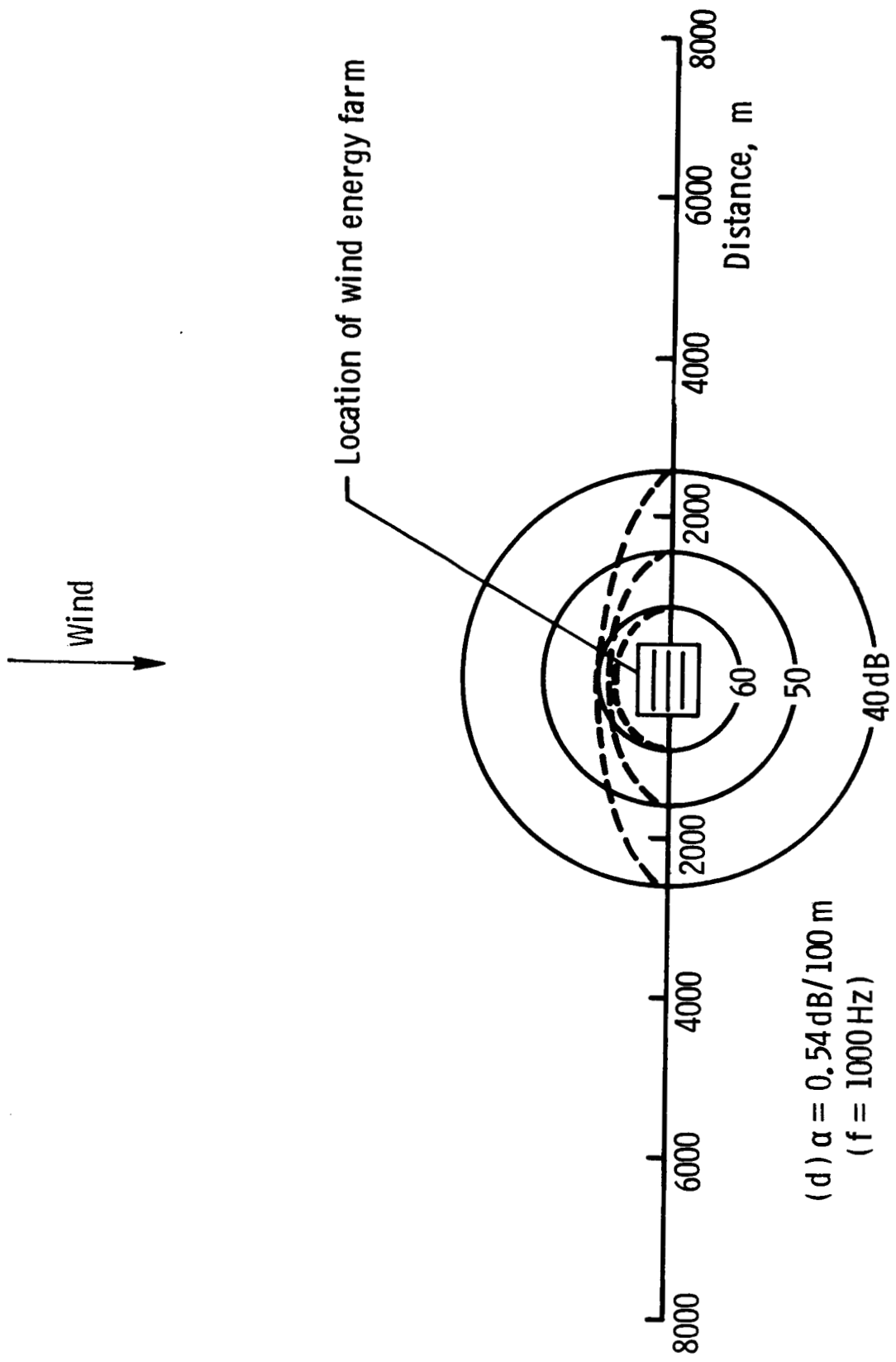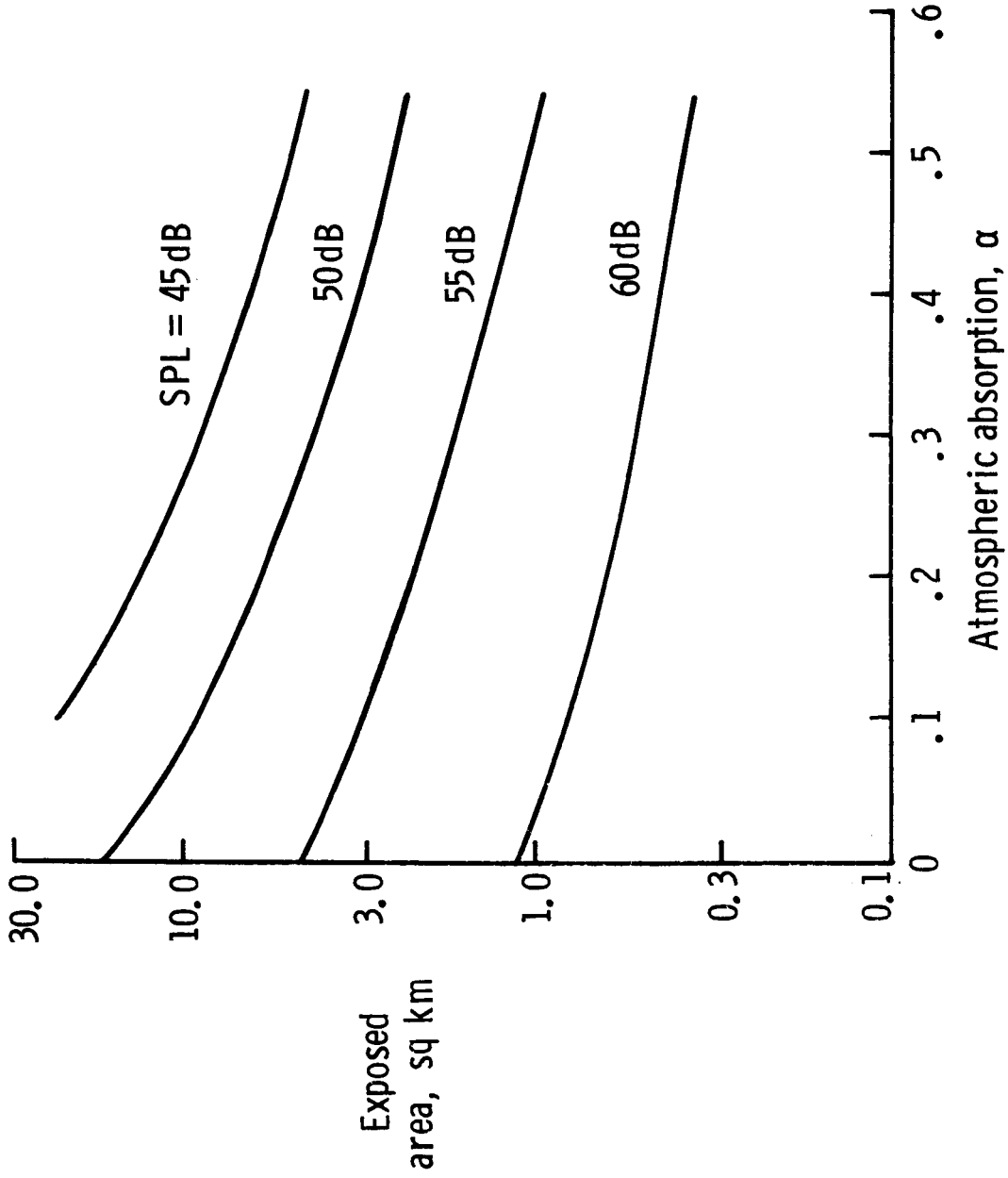(f = 1000 Hz)

Figure 13. – Concluded.

Figure 14. – Ground areas exposed to various maximum values of sound pressure level from wind energy farm configuration A as a function of atmospheric absorption.
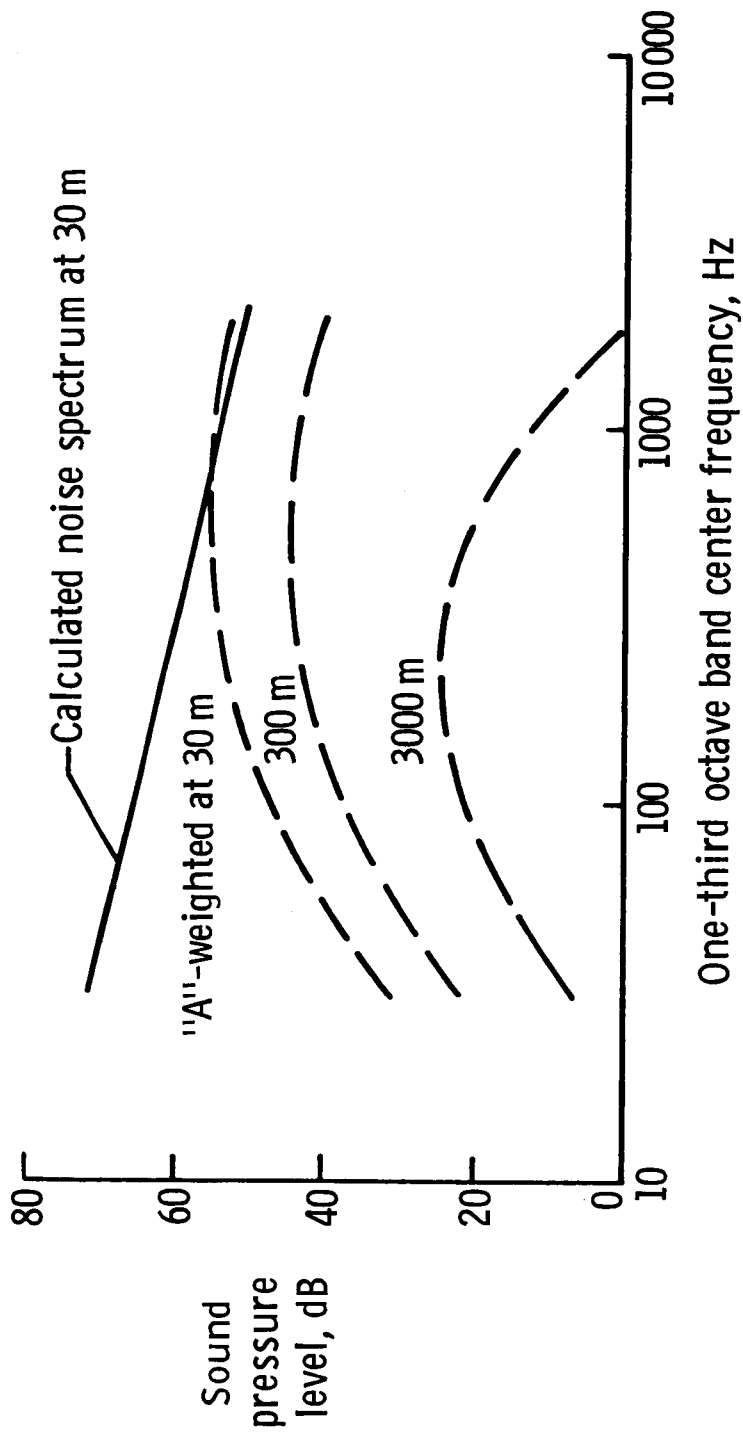
Figure 15. — Estimated "A"-weighted noise spectra at various distances downwind from a wind energy farm corresponding to configuration A.

1. Report No. NASA CR-177956	2. Government Accession No.	3. Recipient's Catalog No.
4. Title and Subtitle Prediction of Far Field Noise from Wind Energy Farms		5. Report Date April 1986
		6. Performing Organization Code
7. Author(s) Kevin P. Shepherd Harvey H. Hubbard		8. Performing Organization Report No.
		10. Work Unit No.
9. Performing Organization Name and Address The Bionetics Corporation 18 Research Drive Hampton, VA 23666		
		11. Contract or Grant No. NAS1-16978
		13. Type of Report and Period Covered NASA Contractor Report
12. Sponsoring Agency Name and Address National Aeronautics and Space Administration Washington, DC 20546		
		14. Sponsoring Agency Code 776-31-41-02 776-31-41-51

15. Supplementary Notes

This report was prepared jointly by Kevin P. Shepherd and Harvey H. Hubbard of the Bionetics Corp. under contract NAS1-16978. Langley Technical Monitor: Clemans A. Powell

16. Abstract

Included in this paper are a review of the basic physical factors involved in making predictions of wind turbine noise; and an approach which allows for differences in the machines, the wind energy farm configurations and propagation conditions. Example calculations are presented to illustrate the sensitivity of the radiated noise to such variables as machine size, spacing and numbers; and such atmosphere variables as absorption (relative humidity and temperature) and wind direction.

Calculated far field distances to particular sound level contours are greater for lower values of atmospheric absorption, for a larger total number of machines, for additional rows of machines and for more powerful machines. At short and intermediate distances, higher sound pressure levels are calculated for closer machine spacings, for more powerful machines, for longer row lengths and for closer row spacings.

17. Key Words (Suggested by Author(s)) Wind Turbine Noise Prediction Parametric Study	18. Distribution Statement Unclassified - Unlimited Subject Category - 71		
19. Security Classif. (of this report) Unclassified	20. Security Classif. (of this page) Unclassified	21. No. of Pages 33	22. Price A03

N-305

1. Report No. NASA CR-177956	2. Government Accession No.	3. Recipient's Catalog No.
4. Title and Subtitle Prediction of Far Field Noise from Wind Energy Farms		5. Report Date April 1986
		6. Performing Organization Code
7. Author(s) Kevin P. Shepherd Harvey H. Hubbard		8. Performing Organization Report No.
		10. Work Unit No.
9. Performing Organization Name and Address The Bionetics Corporation 18 Research Drive Hampton, VA 23666		11. Contract or Grant No. NAS1-16978
		13. Type of Report and Period Covered NASA Contractor Report
12. Sponsoring Agency Name and Address National Aeronautics and Space Administration Washington, DC 20546		14. Sponsoring Agency Code 776-31-41-02 776-31-41-51

15. Supplementary Notes

This report was prepared jointly by Kevin P. Shepherd and Harvey H. Hubbard of the Bionetics Corp. under contract NAS1-16978. Langley Technical Monitor: Clemans A. Powell

16. Abstract

16. Abstract *NAPS are reviewed.*

~~Included in this paper are a review of~~ the basic physical factors involved in making predictions of wind turbine noise *and* an approach which allows for differences in the machines, the wind energy farm configurations and propagation conditions. Example calculations ~~are presented~~ to illustrate the sensitivity of the radiated noise to such variables as machine size, spacing and numbers, and such atmosphere variables as absorption ~~(relative humidity and temperature)~~ and wind direction *are presented.*

It is found that Calculated far field distances to particular sound level contours are greater for lower values of atmospheric absorption, for a larger total number of machines, for additional rows of machines and for more powerful machines. At short and intermediate distances, higher sound pressure levels are calculated for closer machine spacings, for more powerful machines, for longer row lengths and for closer row spacings.

QABA EAK

X NOISE (SOUND)

17. Key Words (Suggested by Author(s)) Wind Turbine *WINDPOWER UTILIZATION, WINDPOWER GENERATORS* Noise Prediction ~~Parametric Study~~ *INDEPENDENT VARIABLES* X *FAR FIELDS* X *NOISE PROPAGATION*	18. Distribution Statement Unclassified - Unlimited Subject Category - 71
19. Security Classif. (of this report) Unclassified	20. Security Classif. (of this page) Unclassified	21. No. of Pages 33	22. Price A03